Spontaneous formation of nanoparticle stripe patterns through dewetting

JIAXING HUANG[1,2]*, FRANKLIN KIM[1,2]*, ANDREA R. TAO[1,2]*, STEPHEN CONNOR[1,2] AND PEIDONG YANG[1,2]†

[1]Department of Chemistry, University of California, Berkeley, California 94720, USA
[2]Materials Science Division, Lawrence Berkeley National Laboratory, Berkeley, California 94720, USA
*These authors contributed equally to this work
†e-mail: p_yang@berkeley.edu

Published online: 13 November 2005; doi:10.1038/nmat1517

Significant advancement has been made in nanoparticle research, with synthetic techniques extending over a wide range of materials with good control over particle size and shape[1–6]. A grand challenge is assembling and positioning the nanoparticles in desired locations to construct complex, higher-order functional structures. Controlled positioning of nanoparticles has been achieved in pre-defined templates fabricated by top–down approaches[7,8]. A self-assembly method, however, is highly desirable because of its simplicity and compatibility with heterogeneous integration processes. Here we report on the spontaneous formation of ordered gold and silver nanoparticle stripe patterns on dewetting a dilute film of polymer-coated nanoparticles floating on a water surface. Well-aligned stripe patterns with tunable orientation, thickness and periodicity at the micrometre scale were obtained by transferring nanoparticles from a floating film onto a substrate in a dip-coating fashion. This facile technique opens up a new avenue for lithography-free patterning of nanoparticle arrays for various applications including, for example, multiplexed surface-enhanced Raman substrates and templated fabrication of higher-order nanostructures.

Research on liquid-supported thin films dates back to the nineteenth century[9]. When amphiphilic molecules (usually dissolved in an immiscible volatile solvent) are spread onto a water surface, a Langmuir–Blodgett thin film[10,11] can be obtained. The film comprises a monolayer of molecules supported on a water subphase. The molecular density of the monolayer can be readily altered by mechanically compressing or expanding the film. The thin film can then be transferred onto a substrate (by dip-coating) whereby a solid-state thin film forms on evaporation of the underlying water layer. This simple and general process has led to numerous applications based on ultrathin films[12–14]. Nanoparticles can also be organized in the same Langmuir–Blodgett fashion to create functional devices. Most research efforts in nanoparticle Langmuir–Blodgett films aim to produce high-density and even close-packed nanoparticle arrays[15–21]. Little has been done to study the low-density nanoparticle monolayers and their transfer

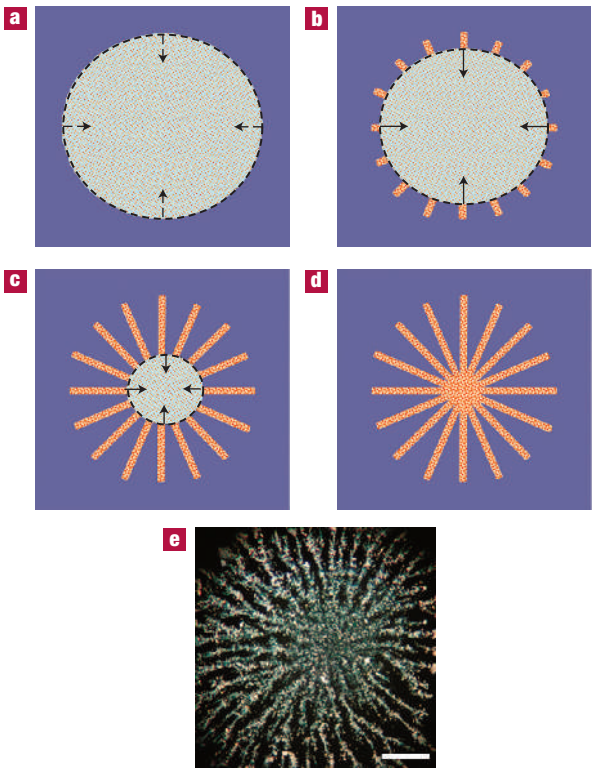

Figure 1 Spoke pattern formation. Schematic drawings illustrating the formation of spoke patterns on dewetting a dilute Langmuir film of gold nanoparticles (gold dots) on hydrophilic SiO_2/Si substrate as observed with an optical microscope. **a**–**e**, At the initial stage (**a**,**b**), the nanoparticles precipitate to form the 'spoke tips' at the rim of the film, which then propagate inwards (**c**,**d**, along the arrows) as the water front (dashed lines) retreats leading to a spoke pattern such as that shown in **e**, an optical microscopy image (scale bar = 200 μm). The propagation of the spokes was captured in the Supplementary Information, Video S1.

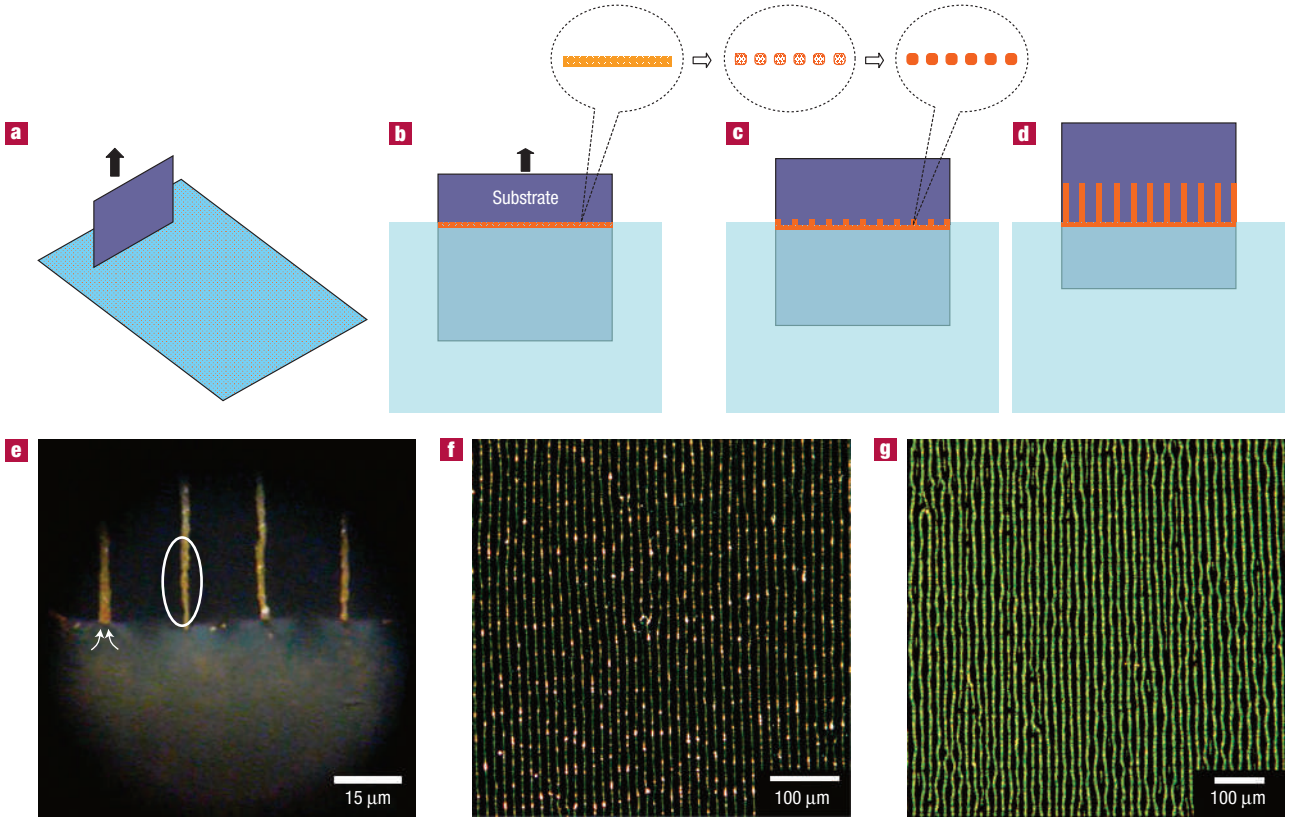

Figure 2 Extended stripe pattern formation through dip-coating. a–d, A schematic drawing illustrating the formation of an aligned gold nanoparticle stripe pattern by vertical deposition (**a**,**b**). Only the nanoparticles at the water–substrate contact line (gold dots in **b–d**) are shown for clarity. The substrate is raised slowly (**a**,**b**) so that water is evaporated when a new surface is exposed. The 'wet' contact line containing uniformly dispersed nanoparticles breaks up into aggregates of nanoparticles (**b**,**c**) owing to the fingering instability during the initial dewetting stage. These fingertips then guide further deposition of nanoparticles, finally forming the extended stripe pattern (**d**). **e**, Direct optical microscopy observation of the water front (see Supplementary Information, Video S2) reveals a rapid motion of nanoparticles towards the wet tips (circled area) of the stripes as indicated by the arrows. This leads to the unidirectional growth of the stripes across the entire substrate as shown in the optical microscopy image in **f**. **g**, Silver nanoparticle stripes have been obtained in the same fashion.

onto substrates. Compared with a close-packed nanoparticle monolayer, the dewetting process of a dilute monolayer should be especially interesting because it allows for a higher degree of convection-induced motion during evaporation. Here, we present our experimental observations on the rearrangement of metal nanoparticles from a dilute monolayer during evaporation. Ordered alignment of nanoparticles at the micrometre scale can be created on a hydrophilic substrate by controlled dewetting of the monolayer.

Gold (~100 nm) and silver (~50 nm) nanoparticles are synthesized through a modified polyol process as reported elsewhere[3,4]. A dilute Langmuir–Blodgett film of these nanoparticles can be readily prepared by spreading a chloroform dispersion onto water. To examine the evaporation-induced assembly process, part of the nanoparticle film was 'scooped' onto an oxide-coated Si wafer (piranha-treated, contact angle $< 20°$), which was then laid horizontally on a flat surface. The nanoparticles settled onto the wafer after the water evaporated. In the dried film, 'spoke'-like radial patterns were observed under an optical microscope (Nikon Optiphot, dark field mode), as shown in Fig. 1e. This type of pattern was formed by the rearrangement of nanoparticles during the drying process, as illustrated in Fig. 1a–d. In the initial dewetting stage, nanoparticles precipitate as aggregated domains along the water–substrate contact line (Fig. 1a,b). These aggregates seemed to serve as nucleation centres to collect extra nanoparticles from the wet particle film as they advance towards the retreating water rim (Fig. 1c). The motion of the gold nanoparticles near these extending finger-like aggregates can be readily observed by means of optical microscopy (see Supplementary Information, Video S1). They seem to be rapidly 'extracted' from the dewetting front, forming the new ends of the elongating finger tips during evaporation. This is probably due to the convective flow of water induced by dewetting. As the stripes propagated inwards, a spoke pattern was constructed when the film was completely dried (Fig. 1d,e). Although a detailed mechanism for this spoke pattern formation is yet to be explored and may be rather complex, an important piece of information is already gained from this simple experimental observation: the orientation of the stripes seems to be normal to the retreating water front. This suggests the possibility of modifying the pattern by tuning the dewetting water front[22,23]. If the dewetting front is regulated, ordered patterns should be obtained.

A very convenient method for controlling the dewetting front is dip-coating (Fig. 2a,b). In dip-coating, the water–substrate contact line is moved across as the SiO_2/Si substrate is slowly pulled up (2 mm min^{-1}, unless otherwise mentioned), collecting the nanoparticles from the air–water interface. The retreating meniscus is determined by the upward movement of the substrate and should be unidirectional. In this manner, we have obtained highly oriented stripe patterns of both gold (Fig. 2f) and silver

(Fig. 2g) nanoparticles. The stripe pattern has uniform thickness and inter-stripe distance over the entire substrate (of the order of cm^2). Although it is difficult to directly observe the stripe formation *in situ* at the contact line, one can foresee that it probably follows the same trend as observed in the spoke pattern formation (Fig. 1). When the substrate is pulled, the nanoparticles at the contact line are carried off the surface film and dried onto the substrate. During this step, the continuous line of nanoparticles at the water–substrate contact line tends to segregate into more concentrated, periodically distributed domains of nanoparticles (Fig. 2b,c) owing to the 'fingering instability' of the drying front[24–27]. The uniform size of these domains is probably due to the local depletion of available nanoparticles at the drying edge. This picture is analogous to uniform crystal growth on periodically placed nuclei[28]. As the substrate continues to be raised, new nanoparticles precipitate out of the Langmuir–Blodgett film; the domains grow into lines as the contact line retreats (Fig. 2d), forming aligned stripes parallel to the pulling direction (Fig. 2f,g).

Occasionally, a pendant water droplet is retained at the bottom edge of the substrate after the entire substrate is raised above the water surface. Monitoring this droplet allows us to visualize the dynamic stripe formation at the edge of the contact line by optical microscopy (see Supplementary Information, Video S2). A snapshot of Video S2 is presented in Fig. 2e, showing the growing ends (circled area) of four adjacent stripes at the rim of the pedant droplet. The stripe tips (still in contact with the water-supported Langmuir–Blodgett film) act as channels for capillary flow, selectively transporting the drying nanoparticles to the wet stripe ends.

Examination of stripe orientation over the entire substrate (Fig. 3a) provides further evidence supporting the fact that the stripes grow normal to the withdrawing water front. The convex meniscus of the water–substrate interface yields a curved contact line across the substrate, with maximum curvature at the substrate sides (region b in Fig. 3a). As a result, the stripes originating from this region are bent accordingly, as shown in the scanning electron microscopy (SEM, JEOL-6340F) image (Fig. 3b). Stripes deposited near the substrate sides (region d in Fig. 3a) also curve towards the edge, as shown in Fig. 3d. In the centre of the wafer, the orientation of the stripes is least affected by the substrate boundaries and, therefore, is almost perfectly parallel to the pulling direction. The dewetting process can also be perturbed by defects on the substrate, leaving behind twisted or branched stripes.

The thickness of the stripes is found to be dependent on the particle density on the water surface. Using a Langmuir–Blodgett trough (Fig. 4e, inset), the particle density in the water-supported film can be readily altered by closing or opening a barrier. When the film is compressed, the particle concentration is increased, which also leads to increased surface pressure, as measured by a tensiometer (NIMA PS4 surface pressure sensor). The change in surface pressure is plotted against the area of the nanoparticle film during compression in Fig. 4. The steady increase of the surface pressure is consistent with the poly(vinyl pyrrolidone) (PVP) coating on the nanoparticles, without which an abrupt jump would be observed in the plot[15,17,18,21]. Well-aligned stripe patterns are obtained from dip-coating only in the low-surface-pressure regime, as shown in the SEM images in Fig. 4a–d. The collected stripes become thicker as the film is compressed. The area of coverage by the stripes is found to be linearly dependent on the particle density of the Langmuir film (Fig. 4f). No significant variation between the particle densities in the stripes is noticed for patterns obtained at different surface pressures. This is in contrast to the strong close-packing tendency observed during the self-assembly of sub-10-nm particles[29]. The SEM images in Supplementary

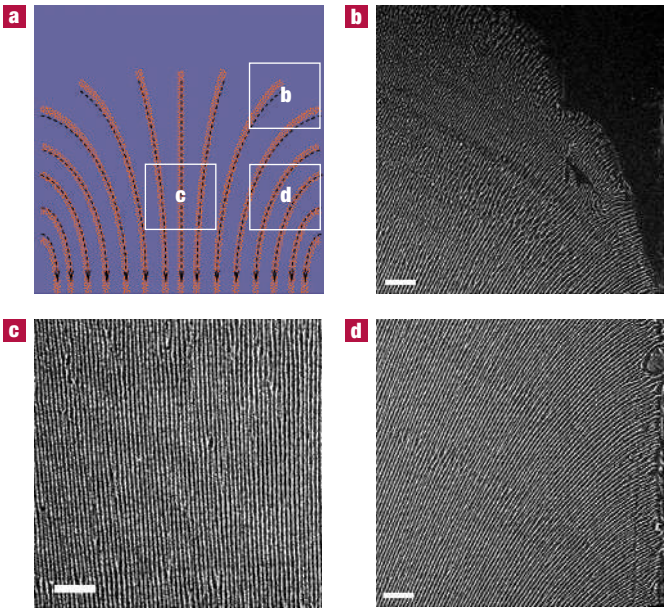

Figure 3 The stripe pattern dictated by the moving contact line. a–d, A schematic drawing (**a**) illustrating the orientation of the stripes at different locations on the substrate as shown in the SEM images (**b–d**). The arrows in **a** indicate the withdrawing direction of the dewetting front as the substrate is raised. The curvature of the stripes at the edges (**b**,**d**) is consistent with the arrows in **a**, suggesting that the propagation of the stripes is normal to the retreating contact line. Scale bars = 100 μm.

Information, Fig. S1 show the distribution of gold nanoparticles inside a stripe pattern collected at 1.5 mN m^{-1} surface pressure. Despite this non-associative arrangement of the nanoparticles, which could be due to the PVP coating on the nanocrystal surface, they do seem to be placed convexly towards the pulling direction. This is consistent with the direction of convective flow that carries the gold nanoparticles (Fig. 2e, Supplementary Information, Videos S1 and S2). The non-uniform block-by-block distribution of particles along the stripes may be a result of an unstable, oscillating wetting front as observed in many surfactant systems[26].

As the stripe pattern is formed during the dewetting process of water on a substrate, the water–substrate interaction should be very important to this dynamic self-assembly process. We have identified the most critical experimental parameter for producing stripe patterns: the concentration of polymer in the water subphase supporting the particle monolayer. As PVP is water soluble, when PVP-coated gold or silver nanoparticles are spread onto the water surface, some PVP molecules may sink into the subphase. The amount of PVP needed to obtain stripe patterns on piranha-treated Si or glass substrates is of the order of 10 μg. This effect is not unique with PVP: other water-soluble polymers, such as polyethylene glycol (PEG, molecular weight $M_w \sim 20{,}000$) can also change the dewetting pattern significantly. Supplementary Information, Fig. S2 shows the effect of PEG concentration on the obtained nanoparticle patterns. This specific gold nanoparticle sample was purified extensively to remove any unbound PVP. Before adding PEG or PVP into the subphase, no stripe pattern was obtained. However, when 10 μg of PEG was added to the subphase, the dispersity of the nanoparticles in the monolayer was significantly improved and highly ordered stripes were obtained. As more PEG (>20 μg) was added, the collected nanoparticle pattern

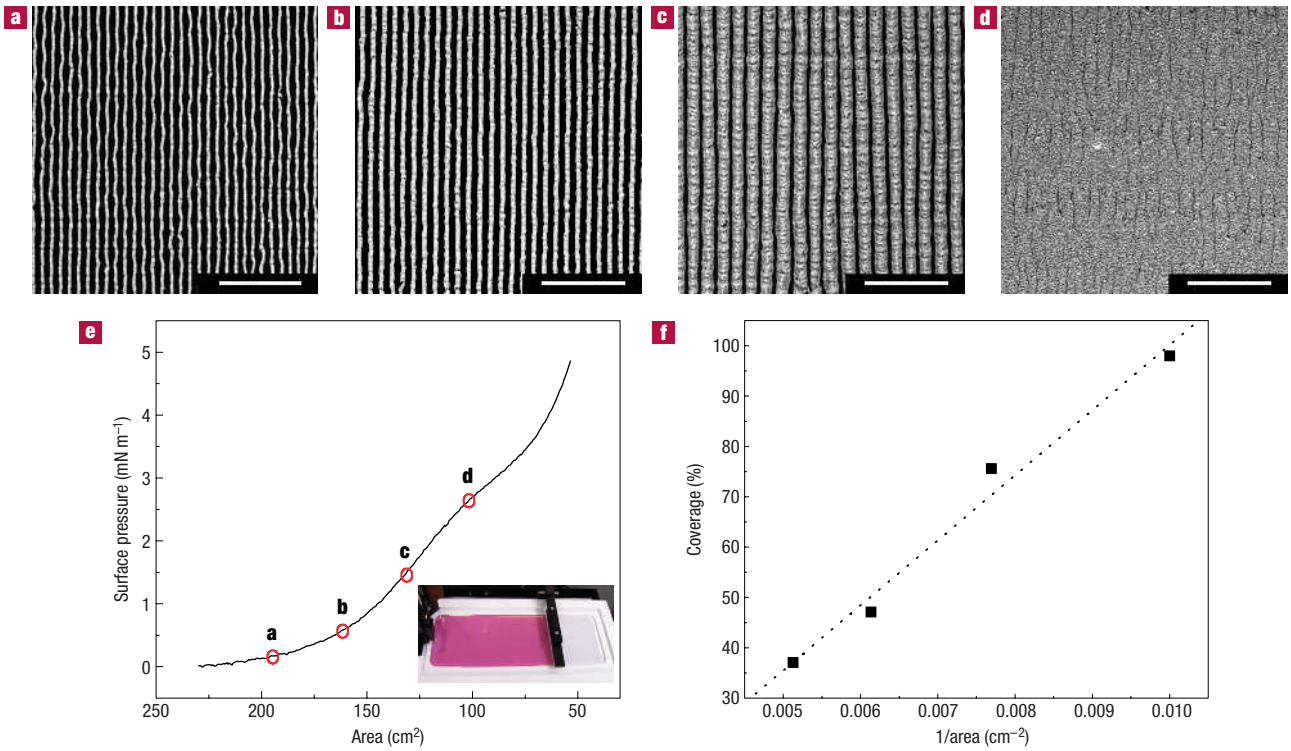

Figure 4 Tuning stripe dimension by changing the surface pressure of the water-supported nanoparticle film. a–d, The SEM images (scale bars = 100 μm) show that the thickness of the stripes increases with higher particle density on water. **e**, The isotherm of the nanoparticle film. The inset shows the typical colour of the gold nanoparticle film on water. **f**, The coverage of the stripes on the substrate is linearly dependent on the particle density of the particle monolayer.

turned into broken stripes and irregular particle islands. The amount of polymer for producing uniform stripes with different nanoparticle samples can thus be conveniently quantified by this serial addition method. We can now make stripe patterns on many different types of substrate by tuning this polymer concentration. These include hydrophilic SiO_2/Si wafers (piranha- or oxygen-plasma-treated, contact angle $< 20°$), glass slides (piranha-treated, contact angle $< 10°$), and even relatively hydrophobic SiO_2/Si wafers (acetone-washed, contact angle $> 60°$). On hydrophobic SiO_2/Si wafers, only segmented stripes (see Supplementary Information, Fig. S3) were obtained, probably owing to unfavourable wetting.

The pulling speed of the substrate is another important factor that can be used to tune the stripe patterns. When ordered stripe patterns are obtained at relatively low pulling speed (<2 mm min^{-1}), their periodicity increases for decreased pulling speed (see Supplementary Information, Fig. S4). Although the optimal pulling speed for producing stripes varies depending on the specific experimental conditions (different particles, substrates and polymer concentrations in the subphase), this trend is generally observed. A similar trend has also been observed in other fluidic systems where fingering instabilities occur at the forced solvent spreading front[30,31]. This observation indicates that it may be possible to tune the periodicity of the stripe pattern independently of the stripe width and spacing. At high pulling speed (>2 mm min^{-1}), the stripes start to lose their integrity. Broken stripes, particle islands and areas of continuous film are usually obtained. This seems to be a result of insufficient drying time, given that a residue water film is often observed on these substrates. The dewetting-induced self-organization of nanoparticles demonstrated here may be a starting point towards inexpensive bottom-up techniques for selective positioning and patterning of nanoparticles over large areas.

METHODS

SYNTHESIS AND PURIFICATION OF GOLD AND SILVER NANOPARTICLES

Gold and silver nanoparticles were prepared based on a modified polyol process as described elsewhere[3,4], using PVP ($M_w \sim 55{,}000$) as the surface-protecting agent and 1,5-pentanediol as both the solvent and reducing agent. Excess PVP and unreacted salts were removed by centrifugation. The surface of the nanoparticles are capped PVP, a commonly used nanoparticle stabilizer, thus rendering their good dispersity in both organic solvents and on a water surface.

PREPARATION OF LANGMUIR–BLODGETT FILMS OF GOLD/SILVER NANOPARTICLES

The purified gold/silver nanoparticles were centrifuged from ethanol and re-dispersed in chloroform by solvent exchange (the estimated particle density was of the order of 10^{12} ml^{-1}). Then a small volume of the chloroform dispersion, typically 1–2 ml, was spread onto a water surface in a rectangular-shaped Teflon trough (NIMA 611D, volume ~200 ml). For gold nanoparticles, a visually continuous pink-coloured film (Fig. 4 inset) can be obtained after 30–60 min.

DIP-COATING ONTO SUBSTRATE

Si wafers with a native oxide layer (typically 1×1 or 1×2 cm^2) were first cleaned with isopropanol by sonication, followed by piranha (30% H_2O_2 + 70% H_2SO_4 by volume) treatment (water contact angle $< 20°$). Similar treatment was carried out for glass slides (contact angle $< 10°$). Relatively hydrophobic Si wafers were obtained by rinsing as-received Si wafers with acetone, followed by isopropanol (contact angle $> 60°$). Before deposition, the substrates were rinsed with water and dried with a N_2 stream. A substrate was then mounted on a dip-coater and dipped into the water subphase. The

dip-coating mechanism on the Langmuir–Blodgett trough has a minimum raising speed of 1 mm min^{-1}. Lower speeds were achieved using a KD100 syringe pump as the motor.

ADDITION OF POLYMER INTO THE SUBPHASE

After a nanoparticle monolayer was formed, a small aliquot (0.1–1 ml) of polymer solution (PVP or PEG, 100 mg l^{-1}) was added into the subphase (~200 ml) from the open side of the Langmuir–Blodgett trough.

Received 29 April 2005; accepted 13 September 2005; published 13 November 2005.

References

1. Ahmadi, T., Wang, Z., Green, T., Henglein, A. & ElSayed, M. Shape-controlled synthesis of colloidal platinum nanoparticles. *Science* **272,** 1924–1926 (1996).
2. Jin, R. *et al.* Photoinduced conversion of silver nanospheres to nanoprisms. *Science* **294,** 1901–1903 (2001).
3. Sun, Y. & Xia, Y. Shape-controlled synthesis of gold and silver nanoparticles. *Science* **298,** 2176–2179 (2002).
4. Kim, F., Connor, S., Song, H., Kuykendall, T. & Yang, P. Platonic gold nanocrystals. *Angew. Chem. Int. Edn* **43,** 3673–3677 (2004).
5. Burda, C., Chen, X., Narayanan, R. & El-Sayed, M. A. Chemistry and properties of nanocrystals of different shapes. *Chem. Rev.* **105,** 1025–1102 (2005).
6. Peng, X. *et al.* Shape control of CdSe nanocrystals. *Nature* **404,** 59–61 (2000).
7. Yin, Y., Lu, Y. & Xia, Y. A self-assembly approach to the formation of asymmetric dimers from monodispersed spherical colloids. *J. Am. Chem. Soc.* **123,** 771–772 (2001).
8. Liddle, J. A., Cui, Y. & Alivisatos, P. Lithographically directed self-assembly of nanostructures. *J. Vac. Sci. Technol. B* **22,** 3409–3414 (2004).
9. Pockels, A. Surface tension. *Nature* **43,** 437–439 (1891).
10. Langmuir, I. & Blodgett, K. B. A new method of investigating unimolecular films. *Kolloid-Zeitschrift* **73,** 258–263 (1935).
11. Blodgett, K. B. Monomolecular films of fatty acids on glass. *J. Am. Chem. Soc.* **56,** 495 (1934).
12. Roberts, G. (ed.) *Langmuir–Blodgett Films* (Plenum, New York, 1990).
13. McCullough, D. H. III & Regen, S. L. Don't forget Langmuir–Blodgett films. *Chem. Commun.* 2787–2791 (2004).
14. Zasadzinski, J. A., Viswanathan, R., Madsen, L., Garnaes, J. & Schwartz, D. K. Langmuir–Blodgett films. *Science* **263,** 1726–1733 (1994).
15. Tao, A. *et al.* Langmuir–Blodgett silver nanowire monolayers for molecular sensing using surface-enhanced Raman spectroscopy. *Nano Lett.* **3,** 1229–1233 (2003).
16. Song, H., Kim, F., Connor, S., Somorjai, G. & Yang, P. Pt nanocrystals: Shape control and Langmuir–Blodgett monolayer formation. *J. Phys. Chem. B* **109,** 188–193 (2005).
17. Yang, P. & Kim, F. Langmuir–Blodgett assembly of one-dimensional nanostructures. *Chem. Phys. Chem.* **3,** 503–506 (2002).
18. Kim, F., Kwan, S., Akana, J. & Yang, P. Langmuir–Blodgett nanorod assembly. *J. Am. Chem. Soc.* **123,** 4360–4361 (2001).
19. Jin, S. *et al.* Scalable interconnection and integration of nanowire devices without registration. *Nano Lett.* **4,** 915–919 (2004).
20. Whang, D., Jin, S., Wu, Y. & Lieber, C. Large-scale hierarchical organization of nanowire arrays for integrated nanosystems. *Nano Lett.* **3,** 1255–1259 (2003).
21. Collier, C. P., Saykally, R. J., Shiang, J. J., Henrichs, S. E. & Heath, J. R. Reversible tuning of silver quantum dot monolayers through the metal–insulator transition. *Science* **277,** 1978–1981 (1997).
22. Sztrum, C. G., Hod, O. & Rabani, E. Self-assembly of nanoparticles in three-dimensions: Formation of stalagmites. *J. Phys. Chem. B* **109,** 6741–6747 (2005).
23. Rabani, E., Reichman, D. R., Geissler, P. L. & Brus, L. E. Drying-mediated self-assembly of nanoparticles. *Nature* **426,** 271–274 (2003).
24. Fitzgerald, S. D. & Woods, A. W. The instability of a vaporization front in hot porous rock. *Nature* **367,** 450–453 (1994).
25. Cazabat, A. M., Heslot, F., Troian, S. M. & Carles, P. Fingering instability of thin spreading films driven by temperature gradients. *Nature* **346,** 824–826 (1990).
26. Gleiche, M., Chi, L. F. & Fuchs, H. Nanoscopic channel lattices with controlled anisotropic wetting. *Nature* **403,** 173–175 (2000).
27. Karthaus, O., Grasjo, L., Maruyama, N. & Shimomura, M. Formation of ordered mesoscopic polymer arrays by dewetting. *Chaos* **9,** 308–314 (1999).
28. Aizenberg, J., Black, A. J. & Whitesides, G. M. Control of crystal nucleation by patterned self-assembled monolayers. *Nature* **398,** 495–498 (1999).
29. Sear, R., Chung, S., Markovich, G., Gelbart, W. & Heath, J. Spontaneous patterning of quantum dots at the air-water interface. *Phys. Rev. E* **59,** R6255–R6258 (1999).
30. Cazabat, A. M., Heslot, F., Troian, S. M. & Carles, P. Fingering instability of thin spreading films driven by temperature-gradients. *Nature* **346,** 824–826 (1990).
31. Purrucker, O., Foertig, A., Luedtke, K., Jordan, R. & Tanaka, M. Confinement of transmembrane cell receptors in tunable stripe micropatterns. *J. Am. Chem. Soc.* **127,** 1258–1264 (2005).

Acknowledgements

We thank R. Fan, H. Yan, T. Kuykendall and P. Pauzauskie for technical assistance and helpful discussions. This work was supported by the National Science Foundation (CAREER) and the Office of Basic Science, Department of Energy. J.H. gratefully acknowledges the Miller Institute for Basic Research in Science for a postdoctoral fellowship. A.R.T. gratefully acknowledges the National Science Foundation for a graduate research fellowship. S.C. gratefully acknowledges a summer undergraduate research fellowship through Center of Integrated Nanomechanical Systems (COINS). We thank the National Center for Electron Microscopy for the use of their facilities.
Correspondence and requests for materials should be addressed to P.Y.
Supplementary Information accompanies this paper on www.nature.com/naturematerials.

Competing financial interests

The authors declare that they have no competing financial interests.